

## Large-deformation plasticity analysis using the edge-based smoothed finite element method

\*J. Liu<sup>1</sup>, Z.Q. Zhang<sup>2</sup>

<sup>1</sup>Department of Mechanical Engineering, National University of Singapore, 117576, Singapore.

<sup>2</sup>Institute of High Performance Computing, Singapore.

\*Corresponding author: nickliujun@gmail.com

### Abstract

An edge-based smoothed finite element method (ES-FEM) using 3-node triangular element was recently proposed to improve the accuracy and convergence rate of the standard finite element method (FEM) for 2D elastic solid mechanics problems. In this research, ES-FEM is extended to the large-deformation plasticity analysis, and a selective edge-based / node-based smoothed finite element (selective ES/NS-FEM) method using 3-node triangular element is adopted to address the volumetric locking problem. Validity of ES-FEM for large-deformation plasticity problem is proved by benchmarks, and numerical examples demonstrate that, the proposed ES-FEM and selective ES/NS-FEM method possess (1) superior accuracy and convergence properties for strain energy solutions comparing to the standard FEM using 3-node triangular element (FEM-T3), (2) better computational efficiency than FEM-T3 and similar computational efficiency as FEM using 4-node quadrilateral element and 6-node quadratic triangular element, (3) a selective ES/NS-FEM method can successfully simulating severe element distortion problem, and address volumetric locking problem in large-deformation plasticity analysis.

**Keywords:** Large-deformation plasticity, Finite element method (FEM), Edge-based smoothed finite element method (ES-FEM), Volumetric locking, Gradient smoothing.

### Introduction

Numerical simulation of finite-deformed material has attracted numerous research efforts. The finite element method (FEM) has been developed during last decades to deal with material and geometric nonlinear problem. Usually, lower order elements, especially 3-node linear triangular element (T3) for 2-D problem and 4-node linear tetrahedron element (T4) for 3-D problem, are attractive in practical engineering problems because of their intrinsic simplicity, easy preprocessing, and lower requirement on solution regularity. However, the use of T3 or T4 element is highly limited in the large deformation plasticity analysis, because of disadvantages such as convergence problem, element distortion and volumetric locking. Therefore, developing techniques to optimize the linear triangular element is a significant job, and lower order elements with superior accuracy and convergence properties are powerful tools for the simulations of contact-impact, crack propagations, material fracturing progressing, large scale multi-physics etc.

In order to overcome the limitations of FEM, various technologies have been proposed. The strain smoothing technique was used for stabilizing the nodal integrated meshfree method (Chen JS, Wu CT et al. 2001) and then applied in the natural element method (Yoo JW, Moran B et al. 2004). Liu et al. has generalized a gradient (strain) smoothing technique (Liu GR 2008) and applied it in general meshfree settings to accommodate discontinuous shape functions (Liu GR 2009). Applying the same technique to the finite element method, an edge-based smoothed finite element method (ES-FEM)(Liu GR, Nguyen-Thoi T et al. 2009) has been formulated based on the gradient (strain) smoothing technique for static, free and forced vibration analyses in 2D plane strain and plane stress problems. The system stiffness matrix of this method is computed using the gradient smoothing technique over the smoothing domains associated with the edges of the element, which endows its superior convergence properties, computational accuracy and efficiency, spatial and temporal stability.

In this paper, the edge-based smoothed finite element (ES-FEM) is extended to be applied for large strain plasticity analysis, and a selective ES/NS-FEM approach is used to address the volumetric locking problem. Compared to standard FEM, this smoothed technique could be able to use fewer elements to get more precise and stable results, and better convergence property; these properties can decrease the computational cost significantly.

## 2. Edge-based smoothed finite element method for finite strain plasticity

### 2.1 Basic ES-FEM theory and formulation

In ES-FEM, the domain discretization is still based on T3 element in standard FEM, but the integration required in the virtual principle is performed based on the smoothing domains associated with the edges instead of on the triangular element in standard FEM. In this method, the closed problem domain  $\Omega$  is divided into  $N_s$  smoothing domains with  $\overline{\Omega} = \bigcup_{k=1}^{N_s} \overline{\Omega}_k^s$  and  $\Omega_i^s \cap \Omega_j^s = 0$  when  $i \neq j$ , where  $N_s$  is the number of smoothing domains equal to the total number of element edges located in the entire problem domain. For triangular elements, the smoothing domain  $\Omega_k^s$  associated with the element edge  $k$  can be created by connecting two endpoints of the edge to centroids of adjacent elements as shown in Fig. 1.

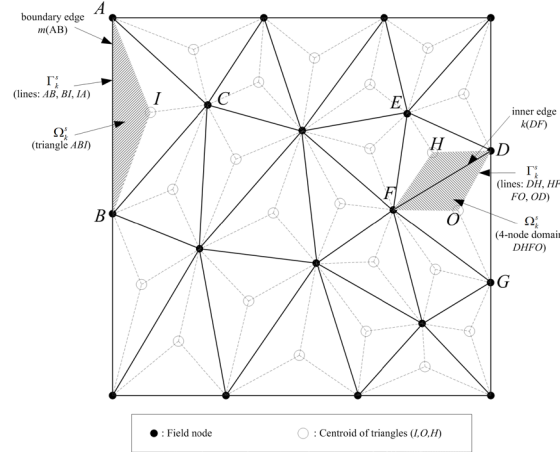


**Fig.1** Triangular elements and the smoothing domains (shaded areas) associated with edges in ES-FEM(Liu GR, Nguyen-Thoi T et al. 2009)

In edge-based smoothing domains, the smoothed gradient of displacement field  $u_i$  can be obtained by

$$\overline{\nabla} u_i = \int_{\Omega_k^s} \nabla u_i(\mathbf{x}) \Phi_k(\mathbf{x}) d\Omega \quad (1)$$

where  $\nabla u_i(\mathbf{x})$  is the gradient of the displacement field  $u_i$ , and  $\overline{\nabla}$  is defined as a *smoothed gradient operator*.  $\Omega_k^s$  is the smoothing domain associated with the edge  $k$ .  $\Phi_k(\mathbf{x})$  is a given smoothing function that satisfies at least unity property

$$\int_{\Omega_k^s} \Phi_k(\mathbf{x}) d\Omega = 1 \quad (2)$$

In ES-FEM, a simple local constant smoothing function can be used in the calculation (Liu GR, Nguyen-Thoi T et al. 2009)

$$\Phi_k(\mathbf{x}) = \begin{cases} 1/A_k^s, & x \in \Omega_k^s \\ 0, & x \notin \Omega_k^s \end{cases} \quad (3)$$

where  $A_k^s$  is the area of the smoothing domain  $\Omega_k^s$ , and is calculated by

$$A_k^s = \int_{\Omega_k^s} d\Omega = \frac{1}{3} \sum_{i=1}^{n_{sd}} A_i^e \quad (4)$$

where  $n_{sd}$  is the number of elements around the edge  $k$  and  $A_k^s$  is the area of the  $j^{th}$  element around the edge  $k$ . Fig.1 shows that  $n_{sd} = 1$  when edge  $k$  is a boundary edge, and  $n_{sd} = 2$  when edge  $k$  is an inside edge.

Using divergence theorem on Eq. (1), it can be obtained that

$$\bar{\nabla} u_i = \frac{1}{A_k^s} \int_{\Gamma_k^s} u_i(\mathbf{x}) \mathbf{n} d\Gamma \quad (5)$$

where  $\mathbf{n}$  is the outward normal vector of the smoothing domain boundary  $\Gamma_k^s$ .

In the ES-FEM-T3, the displacement field is interpolated by the linear FEM shape function, and can be written in the following form

$$u_i = \sum_{I \in G_L} N_I u_{li} \quad (6)$$

where  $N_I$  is the shape function of node  $I$  at reference configuration,  $u_{li}$  is the displacement component of node  $I$ .  $G_L$  is the set of the so-called *supporting nodes* of the smoothing domain  $\Omega_k^s$ . Therefore, the smoothed gradient of displacement field can be formulated by substituting Eq. (6) into (5)

$$\bar{\nabla} u_i = \frac{1}{A_k^s} \int_{\Gamma_k^s} \left( \sum_{I \in G_L} N_I u_{li} \right) \mathbf{n} d\Gamma = \sum_{I \in G_L} \left( \frac{1}{A_k^s} \int_{\Gamma_k^s} N_I \mathbf{n} d\Gamma \right) u_{li} = \sum_{I \in G_L} \bar{b}_{li} u_{li} \quad (7)$$

where  $\bar{b}_{li}$  is the *smoothed derivatives of shape function* as

$$\bar{b}_{li} = \frac{1}{A_k^s} \int_{\Gamma_k^s} N_I n_i d\Gamma \quad (8)$$

Naturally, the smoothed strain  $\bar{\boldsymbol{\varepsilon}}$  in the domain  $\Omega^{(k)}$  associated with edge  $k$  can now be obtained using  $\bar{b}_{li}$

$$\bar{\boldsymbol{\varepsilon}} = \begin{bmatrix} \bar{b}_{lx} & 0 \\ 0 & \bar{b}_{ly} \\ \bar{b}_{ly} & \bar{b}_{lx} \end{bmatrix} \mathbf{u}_I = \bar{\mathbf{B}}_I \mathbf{u}_I \quad (9)$$

## 2.2 Formulating the large deformation plasticity model

In continuum mechanics, the deformation gradient has the form of

$$\mathbf{F} = \nabla \mathbf{u} + \mathbf{I} \quad (10)$$

where  $\mathbf{u}$  is the displacement field tensor,  $\nabla$  is the gradient operator, and  $\mathbf{I}$  is the identity matrix. The *smoothed deformation gradient* associated with edge  $k$  based on the smoothed domain can be defined as:

$$\bar{\mathbf{F}} = \int_{\Omega^{(k)}} \mathbf{F}(X) \Phi_k(X) d\Omega = \frac{1}{A^{(k)}} \int_{\Omega^{(k)}} \mathbf{F}(X) d\Omega = \frac{1}{A^{(k)}} \int_{\Omega^{(k)}} \nabla \mathbf{u} d\Omega + \mathbf{I} \quad (11)$$

Applying divergence theorem to Eq. (11) in the current configuration yields

$$\bar{\mathbf{F}} = \frac{1}{A_k^s} \int_{\Gamma_k^s} \mathbf{u} \otimes \mathbf{n} d\Gamma + \mathbf{I} = \bar{\mathbf{e}} + \mathbf{I} \quad (12)$$

where  $\bar{\mathbf{e}}$  represents the smoothed gradient field of displacement, i.e.  $\bar{\nabla}u_i$  given in Eq. (5).  $\mathbf{n}$  is the outward normal vector. Also, the *smoothed rate of deformation* tensor could be calculated as

$$\bar{\mathbf{L}} = \dot{\bar{\mathbf{F}}}\bar{\mathbf{F}}^{-1} \quad (13)$$

The *smoothed deformation rate* and *smoothed continuum spin* can be additively decomposed as

$$\bar{\mathbf{D}} = \bar{\mathbf{D}}^e + \bar{\mathbf{D}}^p \quad (14)$$

$$\bar{\mathbf{W}} = \bar{\mathbf{W}}^e + \bar{\mathbf{W}}^p = \bar{\mathbf{W}}^e \quad (15)$$

The *smoothed Jaumann stress rate* could be obtained by

$$\bar{\mathbf{T}}^{\nabla} = \kappa \text{tr}(\bar{\mathbf{D}}^e)\mathbf{I} + 2\mu\bar{\mathbf{D}}^e \quad (16)$$

where  $\kappa$  and  $\mu$  are conventional Lamé elastic constants. The  $J_2$  associated flow theory has the form of

$$\bar{\mathbf{D}}^p = \dot{\lambda} \frac{\partial \bar{\mathbf{F}}}{\partial \bar{\mathbf{T}}} \quad (17)$$

where  $\dot{\lambda}$  is the plasticity multiplier. The consistent tangent matrix can be solved by (Zienkiewicz OC and Taylor RL 2000)

$$\mathbf{C}^{ep} = \kappa \mathbf{m} \mathbf{m}^T + 2\mu \left[ \left( 1 - \frac{2\mu\Delta\lambda}{|\bar{\mathbf{T}}^{tr}|} \right) \mathbf{I}_0 - \left( \frac{3\mu}{3\mu + H_i} - \frac{2\mu\Delta\lambda}{|\bar{\mathbf{T}}^{tr}|} \right) \bar{\mathbf{n}} \bar{\mathbf{n}}^T \right] \quad (18)$$

The meaning of parameters mentioned in Eq. (18) can be found in reference (Zienkiewicz OC and Taylor RL 2000).

### 2.3 A smoothing-domain-based selective ES/NS-FEM model for the volume locking problem

In large plasticity deformation problem, the elastic strain could be negligible compared to the plastic strain which does not change the volume of material. Therefore, incompressible deformation may occur in plane strain, axisymmetric, or three dimension problem, and this could probably result in volumetric locking phenomenon in FEM analysis. Traditional ( $u/p$ ) mixed formulations could solve the problem, with increasing of computational cost. Reduced integration is the most common method used in commercial FEM software, however, the developer should be careful about the zero energy modes and it may yield inaccurate result.

Based on these considerations, a combined ES/NS-FEM approach was proposed (Liu GR, Nguyen-Thoi T et al. 2009), which was mainly used to solve the volumetric locking problem when Poisson's ratio approaches to 0.5. In this paper, this method will be extended to the incompressible large deformation plasticity analysis to overcome volumetric locking. For plasticity deformation, the consistent tangent matrix  $\mathbf{C}^{ep}$  in Eq. (18) can be decomposed into two portions - i.e. volumetric and deviatoric parts respectively, as

$$\mathbf{C}^{ep} = \mathbf{C}_{vol}^{ep} + \mathbf{C}_{dev}^{ep} \quad (19)$$

where  $\mathbf{C}_{vol}^{ep}$  is related to the material volume change, and  $\mathbf{C}_{dev}^{ep}$  is corresponding to shape change.

These two matrix can be obtained by

$$\begin{aligned} \mathbf{C}_{vol}^{ep} &= K \mathbf{m} \mathbf{m}^T \\ \mathbf{C}_{dev}^{ep} &= 2\mu \left[ \left( 1 - \frac{2\mu\Delta\lambda}{|\bar{\mathbf{T}}^{tr}|} \right) \mathbf{I}_0 - \left( \frac{3\mu}{3\mu + H_i} - \frac{2\mu\Delta\lambda}{|\bar{\mathbf{T}}^{tr}|} \right) \bar{\mathbf{n}} \bar{\mathbf{n}}^T \right] \end{aligned} \quad (20)$$

In large deformation plasticity,  $\mathbf{C}_{vol}^{ep}$  is significant in FEM simulation. However, it contributes little for the displacement results, because the volume change only occurs in elasticity deformation; this

may result in volume locking. Since node-based smoothing domain used in NS-FEM is effective in overcoming volumetric locking (Liu GR, Nguyen-Thoi T et al. 2009), it is proper to use NS-FEM to calculate the volumetric portion of the stiffness matrix, and ES-FEM to calculate the deviatoric portion of the stiffness matrix. This approach is so-called *selective ES/NS-FEM*.

### 3. Numerical examples

#### 3.1 Plane strain beam bending

A  $0.02\text{m} \times 0.2\text{m}$  beam is fixed on the left side and subjected to a constant downward velocity on the bottom point of the right side as shown in Fig.2. A total displacement of  $0.05\text{m}$  is performed in this problem. The material properties are given as: Young's modulus  $E=120\text{MPa}$ , Poisson's ratio  $\nu=0.3$ , yield stress  $\sigma_y=1\text{MPa}$ . Isotropic hardening with the plasticity modulus  $H_i=1\text{MPa}$ , and plane strain condition is assumed.

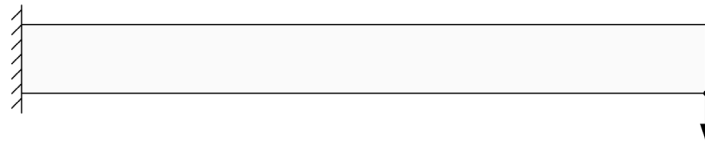


Fig.2 The beam bending problem

Four different methods are used in this case for comparison, i.e. FEM-T3, FEM-Q4, FEM-T6 and ES-FEM. 200 time steps are used in all solutions. Reference solutions are calculated using Abaqus with very fine meshes.

The elastic strain energies are calculated using FEM-T3, FEM-Q4, FEM-T6 and ES-FEM respectively, with different mesh densities and time steps. And the comparison of strain energy convergence with the number of degrees of freedom (DOFs) is plotted in Fig.3. It shows that for the same number of DOFs, the ES-FEM can get result much closer to the reference solution than FEM-T3, i.e. ES-FEM-T3 is much more accurate than FEM-T3. Furthermore, with the increasing of number of DOFs, ES-FEM converges to the reference result much faster than FEM-T3. The FEM-T3 is hardly to converge because it is very stiff. Moreover, ES-FEM-T3 can get similar accurate result compared with FEM using 4-node quadrilateral element and 6-node quadratic triangular element; this is a big advantage for the ES-FEM-T3 technique.

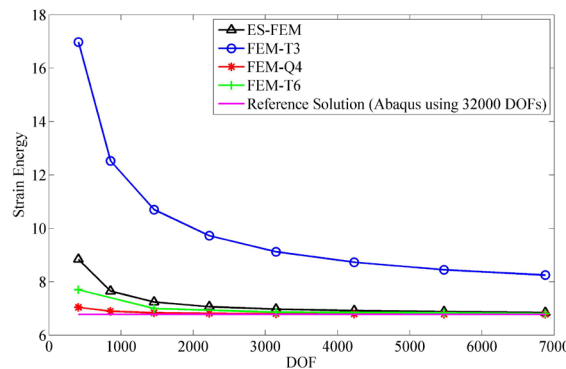
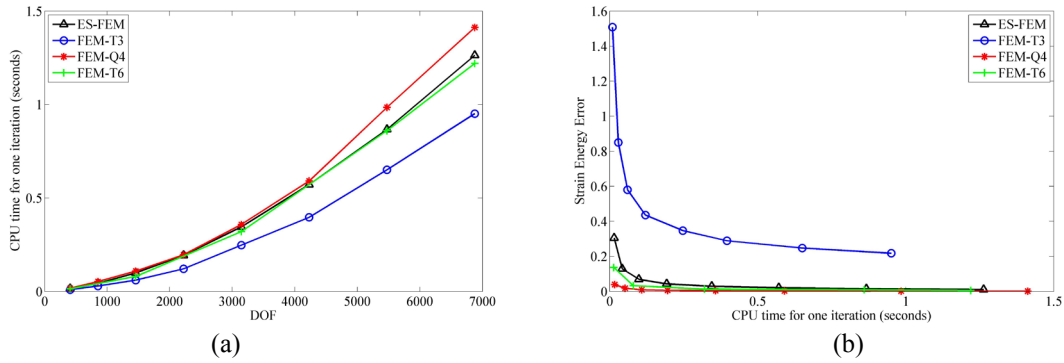


Fig.3 Convergence of the elastic strain energy versus the number of degrees of freedom

Fig.4 compares the computational cost and efficiency of the four different methods for different mesh densities. The CPU time shown in the figure represents the average computational cost for one iteration; this include the time of assembling stiffness matrix and solving linear equations, and it can be calculated by

$$t = \frac{t_{total}}{N_{ite}} \quad (21)$$

where  $t_{total}$  is the total CPU time and  $N_{ite}$  is the number of iterations. Fig.4(a) shows that with the same mesh density, the computational cost of ES-FEM is larger than FEM-T3 and similar as FEM-Q4 and FEM-T6. However, when the computational efficiency (computation time for the same accuracy) is considered, ES-FEM is much more effective than FEM-T3, and could get similar computational efficiency compared to FEM-Q4 and FEM-T6.



**Fig.4** Comparison of the computational cost and efficiency of three different methods  
(a) Computational cost; (b) Computational efficiency

The deformation configurations with effective plastic strain contours for ES-FEM and FEM-Q4 (Abaqus) are plotted in Fig.5, and similar contour profiles are obtained. Fig.5 illustrates that ES-FEM is a valid and effective method in large deformation plasticity analysis.

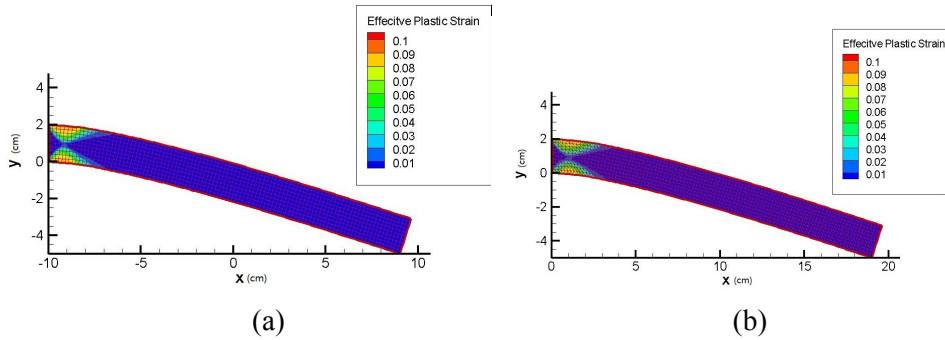


**Fig.5** Effective plastic strain contour using 2222 DOFs (a) FEM-Q4 (Abaqus) and (b) ES-FEM

### 3.2 Downward forging of a billet

A billet is subjected to a constant downward velocity on the top surface as shown in Fig.6(a). The material properties are given as: Young's modulus  $E=200\text{GPa}$ , Poisson's ratio  $\nu=0.49$ , yield stress  $\sigma_Y=500\text{MPa}$ . Isotropic hardening with the plasticity modulus  $H_i=1000\text{MPa}$  and plane strain condition is assumed.

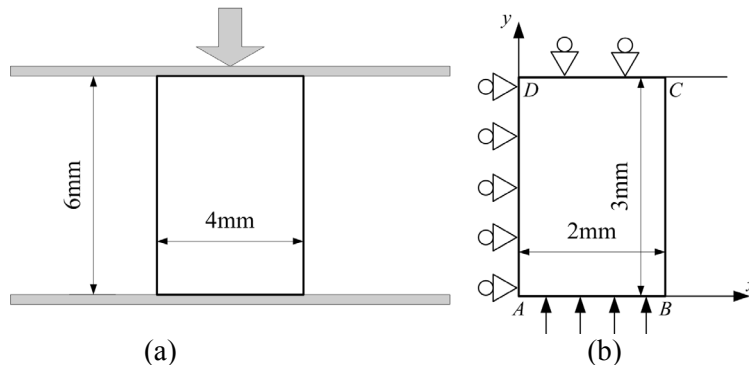


**Fig.6** (a) Compression forging of a billet (b) A quarter symmetrical model for the forging of billet

A quarter symmetrical model and boundary conditions imposed are shown in Fig.6(b). The dies were modeled as being rigid, and no sliding is assumed between the billet and die during contact. Because the material is nearly incompressible ( $\nu = 0.49$ ) and the deformation is very large, the volumetric locking must be considered. Hence the selective ES/NS-FEM technique is used in this simulation. The problem domain is discretized by ES-FEM-T3, ES/NS-FEM-T3, Q4 and T6 elements, as illustrated in Tab.1.

**Tab. 1** Mesh discretization schemes for different methods

	Number of elements	Number of nodes
ES-FEM-T3/ES/NS-FEM-T3	332	192
Q4	150	176
T6	332	715

The solution of FEM-Q4 is given by Abaqus using  $\bar{\beta}$  method, and FEM-T6 is solved using modified formulation provided in Abaqus (Abaqus 2009). At the end of this simulation, ES/NS-FEM and FEM-Q4 are capable to achieve 50% compression, i.e. the displacement of lower edge  $\Delta u = 0.0015\text{m}$ . However, FEM-T6 can only achieve 42% compression, i.e. the displacement of lower edge  $\Delta u = 0.00126\text{m}$  before the element distorted. ES-FEM-T3 cannot get an accurate result because of volumetric locking. The contours of effective plastic strain for different schemes are plotted in Fig.7.

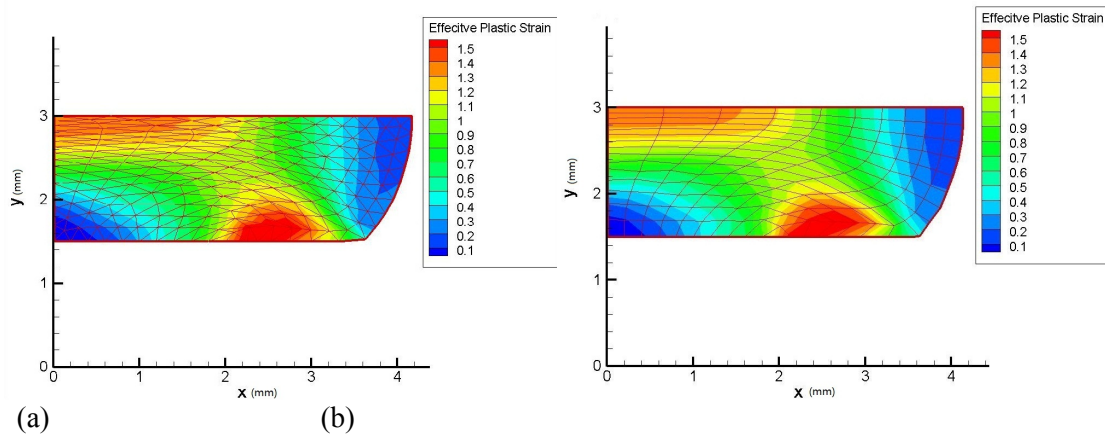


**Fig.7** Solution of forging of billet: deformation configurations  $\Delta u = 1.5\text{mm}$  (50% Compression) solved by (a) Selective ES/NS-FEM-T3, (b) FEM-Q4

Fig.8 plotted the displacement of point C in  $x$  direction by different schemes. It illustrates that the result calculated by ES/NS-FEM-T3 using linear 3-node triangular element agrees very well with FEM-Q4 and FEM-T6, and could bear larger element distortion than FEM-T6. ES-FEM-T3 cannot get a correct result because of volumetric locking, and no locking problem is observed in ES/NS-FEM-T3 approach.

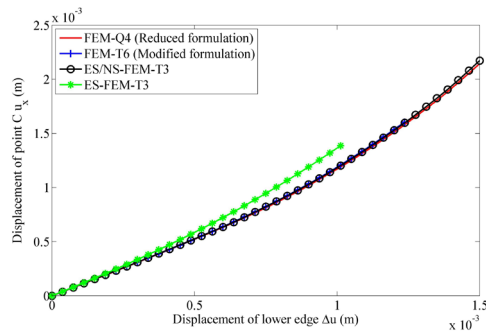


**Fig.8** Displacement solutions of forging of billet at point C

## 4. Conclusion

In order to utilize 3-node linear triangular element for analyzing large strain plasticity problem, an edge-based gradient smoothing technique has been formulated in large deformation plasticity theory. A selective ES/NS-FEM method is also adopted to solve the volumetric locking problem. In this method, the deviatoric portion of tangent modulus is calculated by edge-based smoothed gradient method, and the volumetric portion is solved by node-based smoothed gradient method. Two numerical examples are simulated to show the validity and advantages of ES-FEM compared to standard FEM method. Conclusions could be drawn as follows:

- (1) With the same displacement control, the ES-FEM-T3 can get lower strain energy than the standard FEM with T3 element. This indicates that ES-FEM-T3 is softer than FEM-T3. This property can perfectly alleviate the “over-stiff behavior” of the linear triangular element, and greatly improve the performance of linear triangular element.
- (2) The edge-based smoothing gradient technique can get much more accurate results and faster convergence rate than standard FEM with T3 element. Furthermore, the convergence rate and computing efficiency of ES-FEM using just 3-node element is similar as the standard FEM using 4-node quadrilateral element and 6-node quadratic triangular element.
- (3) Even though only linear triangular element is used, ES/NS-FEM possesses strong capability of handling element distortion. It can sustain larger plastic distortion than FEM-T6 in large strain plasticity analysis.
- (4) No volumetric locking is observed when ES/NS-FEM technique is adopted.

## Reference

- Abaqus (2009). "ABAQUS 6.9-1 Theory manual."
- Chen JS, Wu CT, et al. (2001). "A stabilized conforming nodal integration for Galerkin mesh-free methods." *Int J Numer Methods Eng* **50**(2): 435–466.
- Liu GR (2008). "A generalized gradient smoothing technique and the smoothed bilinear form for Galerkin formulation of a wide class of computational methods." *Int J Comput Methods* **5**(2): 199-236.
- Liu GR (2009). *Mesh free methods: moving beyond the finite element method*. Boca Taton, USA, CRC press.
- Liu GR, Nguyen-Thoi T, et al. (2009). "An edge-based smoothed finite element method (ES-FEM) for static, free and forced vibration analyses of solids." *J Sound Vib* **320**(4-5): 1100-1130.
- Liu GR, Nguyen-Thoi T, et al. (2009). "A node-based smoothed finite element method (NS-FEM) for upper bound solutions to solid mechanics problems." *Comput Struct* **87**(1-2): 14-26.
- Yoo JW, Moran B, et al. (2004). "Stabilized conforming nodal integration in the natural-element method." *Int J Numer Methods Eng* **60**: 861-890.
- Zienkiewicz OC and Taylor RL (2000). *The Finite Element Method: Solid mechanics*, Butterworth-Heinemann.